Letter

Stacked tree construction for free-fermion projected entangled pair states

Yuman He, Kangle Li, Yanbai Zhang, and Hoi Chun Po*
Department of Physics, Hong Kong University of Science and Technology, Clear Water Bay, Hong Kong, China;
IAS Center for Quantum Technologies, Hong Kong University of Science
and Technology, Clear Water Bay, Hong Kong, China;
and Center for Theoretical Condensed Matter Physics, Hong Kong University of Science
and Technology, Clear Water Bay, Hong Kong, China

(Received 16 October 2023; revised 15 January 2024; accepted 29 January 2024; published 17 April 2024)

The tensor network representation of a state in higher dimensions, say a projected entangled-pair state (PEPS), is typically obtained indirectly through variational optimization or imaginary-time Hamiltonian evolution. Here, we propose a divide-and-conquer approach to directly construct a PEPS representation for free-fermion states admitting descriptions in terms of filling exponentially localized Wannier functions. Our approach relies on first obtaining a tree tensor network description of the state in local subregions. Next, a stacking procedure is used to combine the local trees into a PEPS. Lastly, the local tensors are compressed to obtain a more efficient description. We demonstrate our construction for states in one and two dimensions, including the ground state of an obstructed atomic insulator on the square lattice.

DOI: 10.1103/PhysRevResearch.6.L022016

Introduction. Tensor network (TN) representations, like the matrix product state (MPS), provide highly efficient descriptions of quantum many-body states. An MPS is always disconnected when any of its bonds is cut. Physically, this implies the virtual Hilbert space attached to any bond in the network could be given a simple interpretation in terms of the bipartite entanglement of the state [1,2]. This interpretation is valid whenever the tensor network is free of loops, and it has two major consequences. First, a loop-free TN state is *constructible*, in the sense that one could directly construct the TN representation of any given state, up to an error threshold, by successive bipartitions of the system [1–4]. Second, a loop-free TN state is also *computable*, in that there exist canonical forms which enable the numerically exact contraction of TN diagrams arising from, for instance, the computation of physical observables [1,2,5].

Though powerful, the MPS ansatz is natural only for one-dimensional (1D) systems (or as a quasi-1D modeling of higher-dimensional systems). Applying the ansatz in higher dimensions through either a 1D ordering of all the sites [6–8] or through its extension to a tree TN state [9–11], which remains loop-free, would unavoidably assign certain physically neighboring sites to far-apart nodes on the network. Such TNs are generally incompatible with the physical locality of the state and therefore cannot efficiently encode part of the short-range entanglement in the system.

The projected entangled pair state (PEPS) is another natural generalization of MPS to higher dimensions in which physical locality is retained at the cost of introducing loops [2]. As a result, a PEPS is generally neither constructible nor computable: variational optimization or imaginary-time Hamiltonian evolution is needed for finding the PEPS representation of a state, and approximations are invoked in evaluating physical observables through TN contractions [12].

The recent proposal on isometric TN states [13,14] has provided a fruitful avenue for attacking the computability problem of PEPS. Here, we seek to address the complementary problem concerning constructibility, namely, can one obtain a PEPS representation directly from a given state? This question had been answered in the affirmative for the ground states of special models, like those corresponding to stabilizer codes [15–17]. However, for more general problems, indirect approaches like optimization or imaginary-time evolution remain the only tenable options so far. This is true even for free-fermion states, as is reflected in the recent bodies of work concerning fermionic Gaussian TN states [18–23].

In this work, we demonstrate the PEPS constructibility of the ground state of a free-fermion obstructed atomic insulator in two dimensions [24] Our approach follows a divide-and-conquer strategy and consists of three steps, in the order of "tree, stack, and compress." First, we derive the *tree* TN representations for the local descriptions of the state over small open disks. Next, we *stack* the tree TN states to cover the full 2D space. Importantly, the patches overlap and so the resulting TN takes a PEPS form. Lastly, we *compress* the local tensors to obtain an efficient representation. This is achieved by applying MPS techniques to the partial contractions of the TN state along 1D subregions.

We remark that, as a proof of principle, we consider here the ground states of translation-invariant free-fermion Hamiltonians. This allows us to shortcut some of the

*hcpo@ust.hk

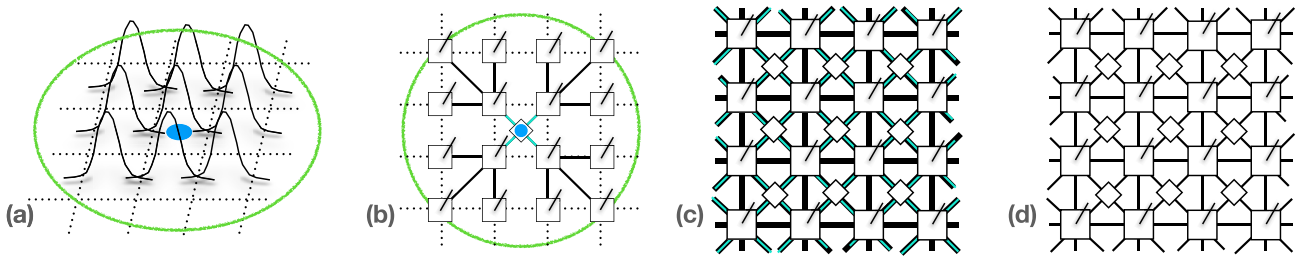

FIG. 1. The overall procedure of the "tree, stack and compress". (a) Exponentially decaying WFs centered at the centers of plaquettes of the square lattice, while atomic sites are the vertices. (b) The tree decomposition of a single WF, where the center of the WF is indicated by a blue dot. The green circle encloses the truncated region for the WF. The dashed lines indicate the square lattice, while the solid lines are legs of the tensors. The legs pointing out-of-page are the physical legs, whereas those in-plane are virtual legs/bonds of local tensors. Blue legs connect the diamond in the center to the neighboring sites, and black legs connect among the square tensors. (c) PEPS obtained by stacking the trees over the whole lattice using translation symmetry. Note that both blue (between square and diamond tensors) and black (among square tensors) are present along the diagonal direction. (d) The local tensors all over the lattice after the compression.

analysis through band-theory techniques like Wannierization. Our approach can be readily generalized to any free-fermion state admitting a (possibly approximate) localized description in terms of filled Wannier functions (WFs). In our current formulation, however, the "stacking" step makes explicit use of the Gaussian nature of the local tensors; generalizing this step to an interacting state is likely nontrivial. Nevertheless, the free-fermion TN representation we constructed could still serve as a natural starting point for constructing an interacting fermionic TN state through, for instance, the Gutzwiller projection [25–28].

Setup. We begin by explaining how our "tree, stack, and compress" steps are carried out for a free-fermion state. We consider a free-fermion Hamiltonian $\hat{H} = \sum_{ij} h_{ij} \hat{c}_i^\dagger \hat{c}_j$, where $\hat{c}_i^\dagger$ and $\hat{c}_i$ are, respectively, the free-fermion creation and annihilation operators. The subscript i denotes possible degrees of freedom, like physical sites, orbitals, etc. The ground state $|\Psi\rangle$ of $\hat{H}$, as is the case for any fermionic Gaussian state, is fully determined by its two-point correlation functions [29,30].

With the number conservation symmetry in our context, we only need to focus on the correlation matrix $C_{ij} = \langle\Psi|\hat{c}_i\hat{c}_j^\dagger|\Psi\rangle$. We further specialize to the case that $\hat{H}$ is translationally invariant and $|\Psi\rangle$ can be obtained by the filling of a full set of WFs, which corresponds to an atomic insulator. The WFs can be viewed as a particularly suitable choice of Fourier transform of the filled Bloch states such that they become exponentially localized in the real space [31]. For an atomic insulator, the WFs can be chosen such that they further respect all the internal and spatial symmetries of the system.

Tree decomposition. Our first step is to obtain a tree TN description for the ground state over a small local subregion. This can be achieved by first focusing on a single WF, which represents a locally defined fermion mode that is occupied in the ground state. Given the exponential localization, the WF can be well-approximated by a truncation to a disk of some radius r_{trunc} which is on the order of its localization length. This is illustrated in Fig. 1(a), where the WF centered at the blue dot is picked, and the truncation is indicated by the green circle.

To obtain a TN representation of the truncated WF, we define a tree which specifies how the sites in the region are to be connected in the TN. For instance, as demonstrated in Fig. 1(b), we can grow a tree with fourfold rotation symmetry on the square lattice.

As a tree is loop-free, we can convert the wave function into a tree TN form by successively applying Schmidt decompositions. More concretely, we view the center site of the tree, which coincides with the center of the WF, as its root. Note that the center need not be occupied by a physical site, and so there may not be a physical leg attached to the center (Fig. 1). Any other sites can be given a height according to its distance from the root. We say two sites belong to the same level if they are equidistant from the root. Starting from the highest level, we perform Schmidt decomposition to obtain the local tensors defined on the sites in the level. Schmidt decompositions within the same level are independent.

For free-fermion states, Schmidt decomposition can be done at the level of correlation matrices, since the reduced density matrix of a subregion is still Gaussian and so it shares the same eigenbasis with the restricted correlation matrix. More explicitly, consider a bipartition of the system into A and B. We can diagonalize the restricted correlation matrices of C as

$$\begin{bmatrix} C_{AA} & C_{AB} \\ C_{AB}^\dagger & C_{BB} \end{bmatrix} = \begin{bmatrix} U_A & \\ & U_B \end{bmatrix} \begin{bmatrix} \Omega_{AA} & \Omega_{AB} \\ \Omega_{AB} & \Omega_{BB} \end{bmatrix} \begin{bmatrix} U_A^\dagger & \\ & U_B^\dagger \end{bmatrix}, \quad (1)$$

where C_{AA}, C_{AB}, and C_{BB} are the corresponding submatrices of C. Ω_{AA} and U_A are, respectively, the eigenvalues and diagonalizing unitary of the restricted correlation matrix C_{AA}; similarly for Ω_{BB} and U_B. Ω_{AB} would generally depend on the arbitrary phases in U_A and U_B [32], but it can be brought into a real diagonal form with non-negative entries through a suitable basis choices [33].

After Schmidt decomposition, one expects to obtain two free-fermion tensors T_A and T_B which can be contracted to reproduce the original state $|\Psi\rangle$. The meaning of a free-fermion tensor, however, is unclear as there will generally be multiple legs with varying number of fermion modes attached to them. For bosonic systems, like qubits, a tensor can always be reinterpreted as a state through a mere reshaping of the legs; for fermions, care must be taken to ensure such reshaping is done in a consistent manner [34]. In our formulation, this is

achieved by purifying all the unitary operators into fermionic Gaussian states defined on a doubled space [35]. In [33], we show how the data contained in Eq. (1) can be packaged into two free-fermion states $|T_A\rangle$ and $|T_B\rangle$, which reproduce $|\Psi\rangle$ upon contraction. This way, all the local tensors can be interpreted as free-fermion states. As such, in the following we use "local tensors" interchangeably with the correlation matrix of its corresponding free-fermion state.

Upon performing all the contractions of the local tensors, as represented by the edges on the tree in Fig. 1(b), we reconstruct the single-particle state given by filling the original (truncated) WF in the current local subregion.

Stacking. To reconstruct the full state $|\Psi\rangle$, we would need to combine the locally defined tree TN states obtained from the individual WFs. Intuitively, we simply need to consider the collection of all the tree TN states, which in our context are related to each other through translation symmetry, and show that these states can be recombined into a single PEPS [Fig. 1(c)]. This step, referred to as the "stacking" procedure, can be achieved as follows. Suppose the local tensor $C^{i,\alpha}$ at site α decomposed from the i^{th} tree is represented as

$$C^{i,\alpha} = \left[\begin{array}{c|c} \Gamma^{i,\alpha}_{\mathrm{pp}} & \Gamma^{i,\alpha}_{\mathrm{pv}} \\ \hline \Gamma^{i,\alpha\,\dagger}_{\mathrm{pv}} & \Gamma^{i,\alpha}_{\mathrm{vv}} \end{array}\right] \tag{2}$$

where the correlation matrix is organized with respect to the physical legs and bonds. Here, i indexes the set of truncated WFs which have support on the site α, and the subscripts p vs v indicate whether the fermion modes are associated with the physical or the virtual legs.

The stacking of the local tensors $C^{i,\alpha}$ for the site α could be expressed as

$$\tilde{C}^{\alpha} = \left[\begin{array}{c|cccc} \sum_{i=1}^{m} \Gamma^{i,\alpha}_{\mathrm{pp}} & \Gamma^{1,\alpha}_{\mathrm{pv}} & \Gamma^{2,\alpha}_{\mathrm{pv}} & \cdots & \Gamma^{m,\alpha}_{\mathrm{pv}} \\ \hline \Gamma^{1,\alpha\,\dagger}_{\mathrm{pv}} & \Gamma^{1,\alpha}_{\mathrm{vv}} & 0 & \cdots & 0 \\ \Gamma^{2,\alpha\,\dagger}_{\mathrm{pv}} & 0 & \Gamma^{2,\alpha}_{\mathrm{vv}} & \ddots & \vdots \\ \vdots & \vdots & \ddots & \ddots & 0 \\ \Gamma^{m,\alpha\,\dagger}_{\mathrm{pv}} & 0 & \cdots & 0 & \Gamma^{m,\alpha}_{\mathrm{vv}} \end{array}\right], \tag{3}$$

where we suppose that there are m trees that contribute to the site α.

Here, the virtual spaces from different trees are independent and so the corresponding parts of their correlation matrices are simply combined as a direct sum. However, all the trees share the same physical Hilbert space at site α and so their contributions add up. As defined, $\tilde{C}^{\alpha}$ is not a proper correlation matrix in general, as the summing procedure defined above does not correspond to any well-defined operations on the Hilbert spaces concerned. Nevertheless, a proper correlation matrix C^{α} can be obtained by the deformation procedure described in [33]. Intuitively, the failure of $\tilde{C}^{\alpha}$ to be a proper correlation matrix stems from the fact that the restrictions of the different trees to the physical Hilbert space of site α lead to modes which are not orthogonal to each other. The deformation process can then be simply interpreted as a suitable orthonormalization step.

We thus obtain a free-fermion PEPS defined by the collection of deformed local tensors. Upon contracting all the virtual legs, we obtain an approximation of the ground state $|\Psi\rangle$.

Compression. The approximate PEPS representation obtained from stacking, however, is far from optimal. In combining the individual trees, we treated their virtual Hilbert spaces as independent. This leads to a superficially high bond dimension which grows as we increase the truncation radius r_{trunc} used in approximating the WFs [33]. As a last step, therefore, we perform a compression of the local tensors.

The idea is that we could first contract the local tensors in one direction to form a free-fermion state defined on an open 1D chain. We can then perform another MPS decomposition of the state while retaining only the most significant virtual modes, which correspond to a truncation to the bond dimension. More concretely, the virtual modes are retained according to their contribution to the von Neumann entanglement entropy: $S = -(\sum_i \omega_i \ln \omega_i + (1-\omega_i)\ln(1-\omega_i))$ [29,36–39], where ω_i corresponds to i^{th} diagonal entry for matrix Ω_{AA} or Ω_{BB} in Eq. (1). To reduce the bond dimension, we drop virtual modes that contribute the least to the entanglement entropy, i.e., we drop the mode i if $\omega_i < \epsilon$ or $\omega_i > 1-\epsilon$ for a prescribed small threshold ϵ. Physically, these dropped virtual modes correspond to degrees of freedom that are well-localized within one side of the entanglement cut, i.e., they do not mediate entanglement across the cut and can therefore be dropped.

After successive Schmidt decomposition, local tensors deeply embedded in a long enough 1D chain should regain bulk properties. Therefore, we choose the local tensor in the middle as the updated C^{α}. Repeating the above process along all possible directions for multiple times, the final fully-compressed C^{α} is obtained, see Fig. 2.

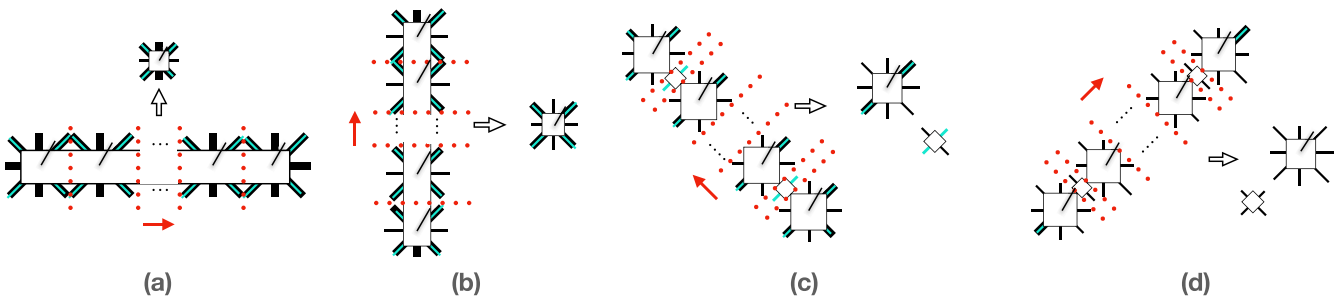

FIG. 2. Compression procedure. The thickness of the legs indicates the size of the bond space. Red dashed lines indicate the successive Schmidt decomposition performed along the red arrow. The hollow arrow points to the final result of each compression step, which is the middle piece among all the decomposed local tensors. The ordering of compression direction is first along (a) horizontal direction, then (b) vertical direction and lastly along the two diagonal directions (c) and (d).

TABLE I. Results for 1D SSH model and 2D OAI model before and after compression. Note that a larger system size is used for the 2D compressed result. The compression thresholds for the 1D and 2D models are respectively $\epsilon = 10^{-6}$ and 10^{-4}.

	1D SSH		2D OAI	
	original	compressed	original	compressed
System Size	100	100	50×50	100×100
r_{trunc}	16		3	
b	$b = 31$	$b = 7$	$b_{\text{v,h}} = 12$; $b_{\text{d}} = 3$	$b_{\text{v,h}} = 5$; $b_{\text{d}} = 3$
$\max_{i,j}(\lvert C_{TN} - C_{\text{exact}}\rvert_{ij})$	6.56×10^{-4}	1.45×10^{-4}	3.16×10^{-3}	4.44×10^{-3}
$(e_{TN} - e_{\text{exact}})/\delta E_{\text{gap}}$	$3.90 \times 10^{-4}\%$	$6.36 \times 10^{-4}\%$	0.17%	0.32%

Examples. We now move on to demonstrating our construction to two obstructed atomic insulator (OAI) systems as a proof of principle. OAI is a special class of atomic insulators for which the centers of the WFs cannot be chosen to coincide with any atomic sites in the system [40].

The 1D Su-Schrieffer-Heeger (SSH) model, one of the most well-known model for a topological insulator, can also be viewed as an OAI if only inversion but not chiral symmetry is retained.

The Hamiltonian for the SSH model is $\hat{H} = \sum_x (t-s)\hat{c}^\dagger_{O_1,x}\hat{c}_{O_2,x} + (t+s)\hat{c}^\dagger_{O_2,x}\hat{c}_{O_1,x+1} + \text{H.c.}$, where t is the uniform hopping parameter, and s is a staggering between intra- and intercell hoppings. O_1 and O_2 are two different orbitals in a unit cell. In the numerics, we choose $t = -1$, $s = 0.1$.

As a second example, we construct an OAI model on the 2D square lattice protected by the four-fold rotation symmetry C_4. We assign three fermion modes, corresponding, respectively, to s, $d_{x^2-y^2}$ and $p_x + ip_y$ atomic orbitals, to each of the sites. Our model is constructed by lowering the energy of a set of nonorthogonal "quasiorbitals" $\hat{f}^\dagger$ which transform differently from all of the atomic orbitals in the system [40–42]. This leads to a band insulator for which the WFs of the filled band are equivalent, symmetry-wise, to the quasiorbitals we started from. More concretely, the Hamiltonian is $\hat{H} = -\sum_{\vec{R}} \eta \hat{f}^\dagger_{\vec{R}} \hat{f}_{\vec{R}}$, where the mode $\hat{f}^\dagger_{\vec{R}}$ is localized to the center of the plaquette in unit cell $\vec{R}$, and transforms trivially under the C_4 rotation symmetry. An atomic insulator obtained by filling s-like WFs localized to the centers of the plaquettes is topologically distant from the innate atomic insulators in the Hilbert space, and so this Hamiltonian serves as an OAI model [33]. In the numerical calculation, we set $\eta = 2$.

The main results are tabulated in Table I. The number of fermion modes attached to a virtual leg is denoted by b. For the 2D model (Fig. 1), we distinguish the vertical/horizontal bond $b_{\text{v,h}}$ and the diagonal bond b_{d} for each square tensor. Before and after compression, we compare the difference between the correlation reproduced from PEPS C_{TN} and the exact through the entry-wise maximum difference $\max_{i,j}(\lvert C_{\text{TN}} - C_{\text{exact}}\rvert_{ij})$. Small values of this difference, on the order of 10^{-3}, were found, and so the exact and TN results are indiscernible in Figs. 3 and 4. We also compare the relative difference of ground state energy density, defined as $(e_{\text{TN}} - e_{\text{exact}})/\delta E_{\text{gap}}$ where e_{TN} and e_{exact} are ground state energy density per unit cell obtained from TN representation and exact calculations respectively. δE_{gap} is the minimal gap over the first Brillouin zone.

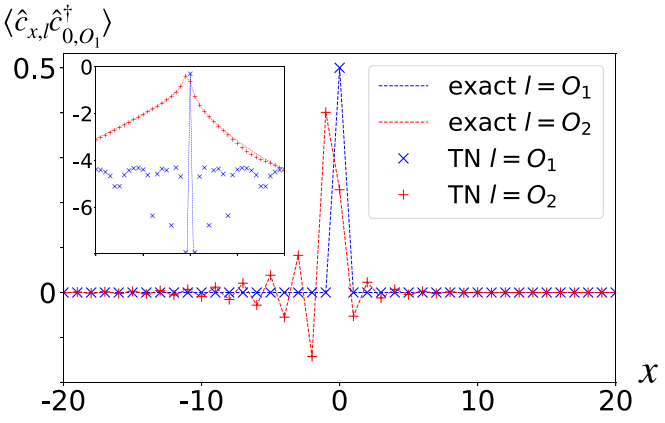

FIG. 3. Correlation function $\langle \hat{c}_{x,l}\hat{c}^\dagger_{0,O_1}\rangle$ for a 100-site SSH model. Only data inside the range $(-20, 20)$ is shown as the values are practically zero outside of this range. The blue and red colors represent the two orbitals O_1 and O_2, respectively. The dashed lines represent exact values while the markers represent the compressed ones obtained from the constructed TN. The inset is the log scale plot of the same range while the vertical axis being $\log_{10}|\langle \hat{c}_{x,l}\hat{c}^\dagger_{0,O_1}\rangle|$.

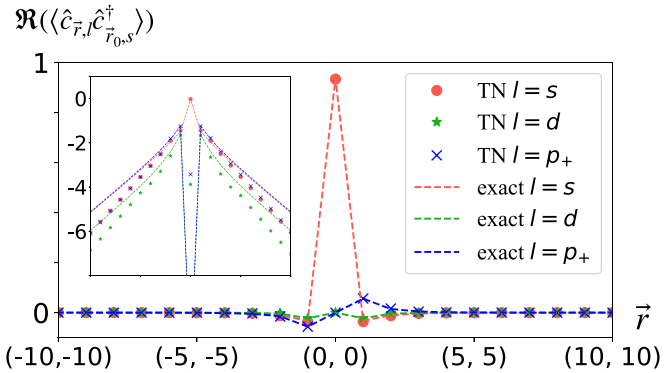

FIG. 4. Real part of correlation function $\Re(\langle \hat{c}_{\vec{r},l}\hat{c}^\dagger_{\vec{r}_0,s}\rangle)$ on a 100×100 square lattice, where $\vec{r}_0 = (0, 0)$. Data for $\vec{r}$ along direction [11] within the range $(-10, 10)$ and $(10, 10)$ is demonstrated. $\Re(\langle \hat{c}_{\vec{r},l}\hat{c}^\dagger_{\vec{r}_0,s}\rangle)$ is practically 0 for $\vec{r}$ outside the region. The red, green, and blue colors represent the s, $d_{x^2-y^2}$ and $p_+ = p_x + ip_y$ orbitals, respectively. The dashed lines are for exact values and the markers show the reconstructed results obtained from our TN. The inset is the log scale plot within the same range while the vertical axis is for $\log_{10}|\Re(\langle \hat{c}_{\vec{r},l}\hat{c}^\dagger_{\vec{r}_0,s}\rangle)|$.

Discussion. In this work, we present a general scheme for constructing PEPS for free-fermion states arising from the filling of exponentially localized WFs. As a proof of principle, we demonstrate our approach for models in one and two dimensions.

Although translation invariance was used to simplify the computation, our approach can be generalized to a strictly real-space formulation for more general systems with incommensurate order or disorder. Interaction effects could also be incorporated by combining the free-fermion TN state with, for instance, Gutzwiller projectors [25–27]. In closing, we remark that, in the restricted context of free-fermion states, there might be tantalizing connections between our construction and a tensor-network-based solution to the quantum marginal problem [43–49]: data confined to small local subregions are first handled by tree TN states, which are then patched into the full pure state through the stacking step. It is an interesting question to consider how our approach might be generalized to attack the corresponding many-body problem.

Acknowledgments. This work is supported by the National Key R&D Program of China (Grant No. 2021YFA1401500) and the Hong Kong Research Grant Council (ECS 26308021).

[1] U. Schollwöck, The density-matrix renormalization group in the age of matrix product states, Ann. Phys. **326**, 96 (2011).
[2] R. Orús, A practical introduction to tensor networks: Matrix product states and projected entangled pair states, Ann. Phys. **349**, 117 (2014).
[3] G. Vidal, Efficient classical simulation of slightly entangled quantum computations, Phys. Rev. Lett. **91**, 147902 (2003).
[4] G. Vidal, Efficient simulation of one-dimensional quantum many-body systems, Phys. Rev. Lett. **93**, 040502 (2004).
[5] S. R. White, Density matrix formulation for quantum renormalization groups, Phys. Rev. Lett. **69**, 2863 (1992).
[6] S. Liang and H. Pang, Approximate diagonalization using the density matrix renormalization-group method: A two-dimensional-systems perspective, Phys. Rev. B **49**, 9214 (1994).
[7] T. Xiang, J. Lou, and Z. Su, Two-dimensional algorithm of the density-matrix renormalization group, Phys. Rev. B **64**, 104414 (2001).
[8] E. Stoudenmire and S. R. White, Studying two-dimensional systems with the density matrix renormalization group, Annu. Rev. Condens. Matter Phys. **3**, 111 (2012).
[9] V. Murg, F. Verstraete, Ö. Legeza, and R. M. Noack, Simulating strongly correlated quantum systems with tree tensor networks, Phys. Rev. B **82**, 205105 (2010).
[10] Y.-Y. Shi, L.-M. Duan, and G. Vidal, Classical simulation of quantum many-body systems with a tree tensor network, Phys. Rev. A **74**, 022320 (2006).
[11] L. Tagliacozzo, G. Evenbly, and G. Vidal, Simulation of two-dimensional quantum systems using a tree tensor network that exploits the entropic area law, Phys. Rev. B **80**, 235127 (2009).
[12] N. Schuch, M. M. Wolf, F. Verstraete, and J. I. Cirac, Computational complexity of projected entangled pair states, Phys. Rev. Lett. **98**, 140506 (2007).
[13] M. P. Zaletel and F. Pollmann, Isometric tensor network states in two dimensions, Phys. Rev. Lett. **124**, 037201 (2020).
[14] M. S. J. Tepaske and D. J. Luitz, Three-dimensional isometric tensor networks, Phys. Rev. Res. **3**, 023236 (2021).
[15] N. Schuch, I. Cirac, and D. Pérez-García, PEPS as ground states: Degeneracy and topology, Ann. Phys. **325**, 2153 (2010).
[16] F. Verstraete, M. M. Wolf, D. Perez-Garcia, and J. I. Cirac, Criticality, the area law, and the computational power of projected entangled pair states, Phys. Rev. Lett. **96**, 220601 (2006).
[17] H. He, Y. Zheng, B. A. Bernevig, and N. Regnault, Entanglement entropy from tensor network states for stabilizer codes, Phys. Rev. B **97**, 125102 (2018).
[18] C. V. Kraus, N. Schuch, F. Verstraete, and J. I. Cirac, Fermionic projected entangled pair states, Phys. Rev. A **81**, 052338 (2010).
[19] T. B. Wahl, H.-H. Tu, N. Schuch, and J. I. Cirac, Projected entangled-pair states can describe chiral topological states, Phys. Rev. Lett. **111**, 236805 (2013).
[20] Q. Mortier, N. Schuch, F. Verstraete, and J. Haegeman, Tensor networks can resolve Fermi surfaces, Phys. Rev. Lett. **129**, 206401 (2022).
[21] J. Dubail and N. Read, Tensor network trial states for chiral topological phases in two dimensions and a no-go theorem in any dimension, Phys. Rev. B **92**, 205307 (2015).
[22] N. Schuch and B. Bauer, Matrix product state algorithms for Gaussian fermionic states, Phys. Rev. B **100**, 245121 (2019).
[23] S. Boutin and B. Bauer, Quantum impurity models using superpositions of fermionic Gaussian states: Practical methods and applications, Phys. Rev. Res. **3**, 033188 (2021).
[24] By a "free-fermion" state, we refer to a fermionic Gaussian state with a definite particle number.
[25] Q. Yang, X.-Y. Zhang, H.-J. Liao, H.-H. Tu, and L. Wang, Projected d-wave superconducting state: A fermionic projected entangled pair state study, Phys. Rev. B **107**, 125128 (2023).
[26] J.-W. Li, J. von Delft, and H.-H. Tu, U(1)-symmetric Gaussian fermionic projected entangled paired states and their Gutzwiller projection, Phys. Rev. B **107**, 085148 (2023).
[27] S. Yang, T. B. Wahl, H.-H. Tu, N. Schuch, and J. I. Cirac, Chiral projected entangled-pair state with topological order, Phys. Rev. Lett. **114**, 106803 (2015).
[28] Y.-H. Wu, L. Wang, and H.-H. Tu, Tensor network representations of parton wave functions, Phys. Rev. Lett. **124**, 246401 (2020).
[29] I. Peschel and V. Eisler, Reduced density matrices and entanglement entropy in free lattice models, J. Phys. A **42**, 504003 (2009).
[30] S. Bravyi, Lagrangian representation for fermionic linear optics, Quantum Info. Comput. **5**, 216 (2005).
[31] N. Marzari, A. A. Mostofi, J. R. Yates, I. Souza, and D. Vanderbilt, Maximally localized wannier functions: Theory and applications, Rev. Mod. Phys. **84**, 1419 (2012).
[32] More generally, basis choice within degenerate subspaces of the singular values.
[33] See Supplemental Material at http://link.aps.org/supplemental/10.1103/PhysRevResearch.6.L022016 for details of the constructed models and operations on fermionic Gaussian states.
[34] Mapping the fermion problem to a bosonic one is one possible (and perhaps standard) way, but this would invoke unwieldy Jordan-Wigner strings and does not manifestly preserve the free-fermion nature of the present problem. While this problem is arguably mild for an MPS or a tree TN, it is much more severe

for the subsequent steps in our problem concerning a 2D state. As such, a fully fermionic formulation is desired, as we discuss in Supplemental Material [33].

[35] M. A. Nielsen and I. L. Chuang, *Quantum Computation and Quantum Information: 10th Anniversary Edition* (Cambridge University Press, Cambridge, 2010).

[36] J. I. Latorre and A. Riera, A short review on entanglement in quantum spin systems, J. Phys. A **42**, 504002 (2009).

[37] G. Vidal, J. I. Latorre, E. Rico, and A. Kitaev, Entanglement in quantum critical phenomena, Phys. Rev. Lett. **90**, 227902 (2003).

[38] J. I. Latorre, E. Rico, and G. Vidal, Ground state entanglement in quantum spin chains, Quantum Info. Comput. **4**, 48 (2004).

[39] M. T. Fishman and S. R. White, Compression of correlation matrices and an efficient method for forming matrix product states of fermionic Gaussian states, Phys. Rev. B **92**, 075132 (2015).

[40] Y. Xu, L. Elcoro, Z.-D. Song, M. G. Vergniory, C. Felser, S. S. P. Parkin, N. Regnault, J. L. Mañes, and B. A. Bernevig, Filling-enforced obstructed atomic insulators, arXiv:2106.10276.

[41] H. C. Po, A. Vishwanath, and H. Watanabe, Symmetry-based indicators of band topology in the 230 space groups, Nat. Commun. **8**, 50 (2017).

[42] B. Bradlyn, L. Elcoro, J. Cano, M. G. Vergniory, Z. Wang, C. Felser, M. I. Aroyo, and B. A. Bernevig, Topological quantum chemistry, Nature (London) **547**, 298 (2017).

[43] A. M. Alhambra and J. I. Cirac, Locally accurate tensor networks for thermal states and time evolution, PRX Quantum **2**, 040331 (2021).

[44] Y. Huang, Computing energy density in one dimension, arXiv:1505.00772.

[45] N. Schuch and F. Verstraete, Matrix product state approximations for infinite systems, arXiv:1711.06559.

[46] A. M. Dalzell and F. G. S. L. Brandão, Locally accurate MPS approximations for ground states of one-dimensional gapped local Hamiltonians, Quantum **3**, 187 (2019).

[47] Y. Huang, Approximating local properties by tensor network states with constant bond dimension, arXiv:1903.10048.

[48] I. H. Kim, Entropy scaling law and the quantum marginal problem, Phys. Rev. X **11**, 021039 (2021).

[49] I. H. Kim, Entropy scaling law and the quantum marginal problem: simplification and generalization, arXiv:2109.11688.